Candidate Hypervelocity Red Clump Stars in the Galactic Bulge Found Using the VVV and *Gaia* Surveys[*]

Alonso Luna[1,2] , Dante Minniti[2,3,4] , and Javier Alonso-García[3,5]

[1] Instituto de Astronomía, Universidad Nacional Autónoma de México, Ciudad Universitaria, 04510, México; aluna@astro.unam.mx
[2] Depto. de Ciencias Físicas, Facultad de Ciencias Exactas, Universidad Andres Bello, Av. Fernandez Concha 700, Las Condes, Santiago, Chile
[3] Millennium Institute of Astrophysics, Av. Vicuna Mackenna 4860, 782-0436, Santiago, Chile; vvvdante@gmail.com
[4] Vatican Observatory, V-00120 Vatican City State, Italy
[5] Centro de Astronomía (CITEVA), Universidad de Antofagasta, Av. Angamos 601, Antofagasta, Chile; javier.alonso@uantof.cl

Abstract

We propose a new way to search for hypervelocity stars (HVS) in the Galactic bulge, by using red clump (RC) giants, that are good distance indicators. The second *Gaia* Data Release and the near-IR data from the VISTA Variables in the Via Lactea (VVV) Survey led to the selection of a volume limited sample of 34 bulge RC stars. A search in this combined data set leads to the discovery of seven candidate hypervelocity red clump stars in the Milky Way bulge. Based on this search we estimate the total production rate of hypervelocity RC stars from the central supermassive black hole (SMBH) to be $N_{\mathrm{HVRC}} = 3.26 \times 10^{-4}$ yr^{-1}. This opens up the possibility of finding larger samples of HVS in the Galactic bulge using future surveys, closer to their main production site, if they originated from interactions of binaries with the central SMBH.

1. Introduction

Hypervelocity stars (HVS) are rare objects that appear to be unbound from the Galaxy. For an authoritative and broad discussion about these objects see Brown (2015). We concentrate on the HVS coming from the Galactic center, produced by the interaction of the central supermassive black hole (SMBH) with a binary system (Hills 1988). The Galactic bulge in particular is the region where one expects to find the highest density of HVS produced by the suspected SMBH at the center of our Galaxy.

Since the first discovery by Brown et al. (2005), quite a few HVS have been found in the Milky Way halo with typical velocities ~1000 km s^{-1} (e.g., Brown et al. 2008, 2014, 2018; Heber et al. 2008; Kollmeier et al. 2009; Kenyon et al. 2014; Palladino et al. 2014; Brown 2015; Geier et al. 2015), and also in the Magellanic Clouds (e.g., Przybilla et al. 2008; Lennon et al. 2017).

In order to explain the ejection process, different model predictions have been made besides the Hills one; Yu & Tremaine (2003) proposed a binary massive BH and a single star ejection mechanism; a globular cluster and an SMBH scenario was introduced by Fragione et al. (2017) and a few others have been introduced by other authors (e.g., Baumgardt et al. 2006; Silk et al. 2012; Zhang et al. 2013; Kenyon et al. 2014; Rossi et al. 2014; Fragione & Loeb 2017; Boubert et al. 2018; Irrgang et al. 2018; Marchetti et al. 2018).

On the basis of these previous studies, it has been estimated that every ~10,000 yr one star is ejected by binary interaction with the Galactic nuclear BH (Sag A*) as an HVS. If we can measure time of ejection, then we can check for bursts due to the accretion of a star cluster by the central SMBH, for example (Capuzzo-Dolcetta & Fragione 2015; Fragione & Capuzzo-Dolcetta 2016).

In this paper we propose a new way to search for HVS in the Galactic bulge. We use the *Gaia* DR2 sample combined with the VVV sample to select bulge RC stars and search for HVS, reporting the discovery of two candidate hypervelocity RC stars in the Galactic bulge.

2. The *Gaia* and VVV Data

Because of the large nonuniform reddening in the bulge fields studied here (e.g., Schlafly et al. 2011; González et al. 2012; Minniti et al. 2016, 2018; Alonso-García et al. 2017, 2018), we use the combination of optical *Gaia* data with near-IR VVV data.

The *Gaia* second data release (DR2) contains data collected between 2014 July and 2016 May (Gaia Collaboration 2018). It improves the photometric and astrometric measurements of the first release (DR1) as well as information on astrophysical parameters, variability, and median radial velocities for some sources. Gaia DR2 contains the apparent brightness in G magnitude for more than 1.6×10^9 sources brighter than 21 mag and, for 1.4×10^9 sources, broadband colors G_{BP} (330–680 nm) and G_{RP} (630–1050 nm), which were not available in DR1. The proper motion (PM) components in equatorial coordinates are available for 1.3×10^9 sources with an accuracy of 0.06 mas yr^{-1} for sources brighter than $G = 15$ mag, 0.2 mas yr^{-1} for sources with $G = 17$ mag and 1.2 mas yr^{-1} for sources with $G = 20$ mag (Gaia Collaboration 2018). The data have been processed by the *Gaia* Data Processing and Analysis Consortium.

The VVV survey maps the Galactic bulge and southern disk in the near-IR with the VIRCAM (VISTA InfraRed CAMera) at the 4.1 m wide-field Visible and Infrared Survey Telescope for Astronomy (VISTA, Emerson & Sutherland 2010) at ESO Paranal Observatory (Minniti et al. 2010; Saito et al. 2012). In the Galactic bulge, the VVV Survey covered 300 sq.deg. (within $-10° < l < 10°$, $-10° < b < 5°$), using the near-IR passbands:
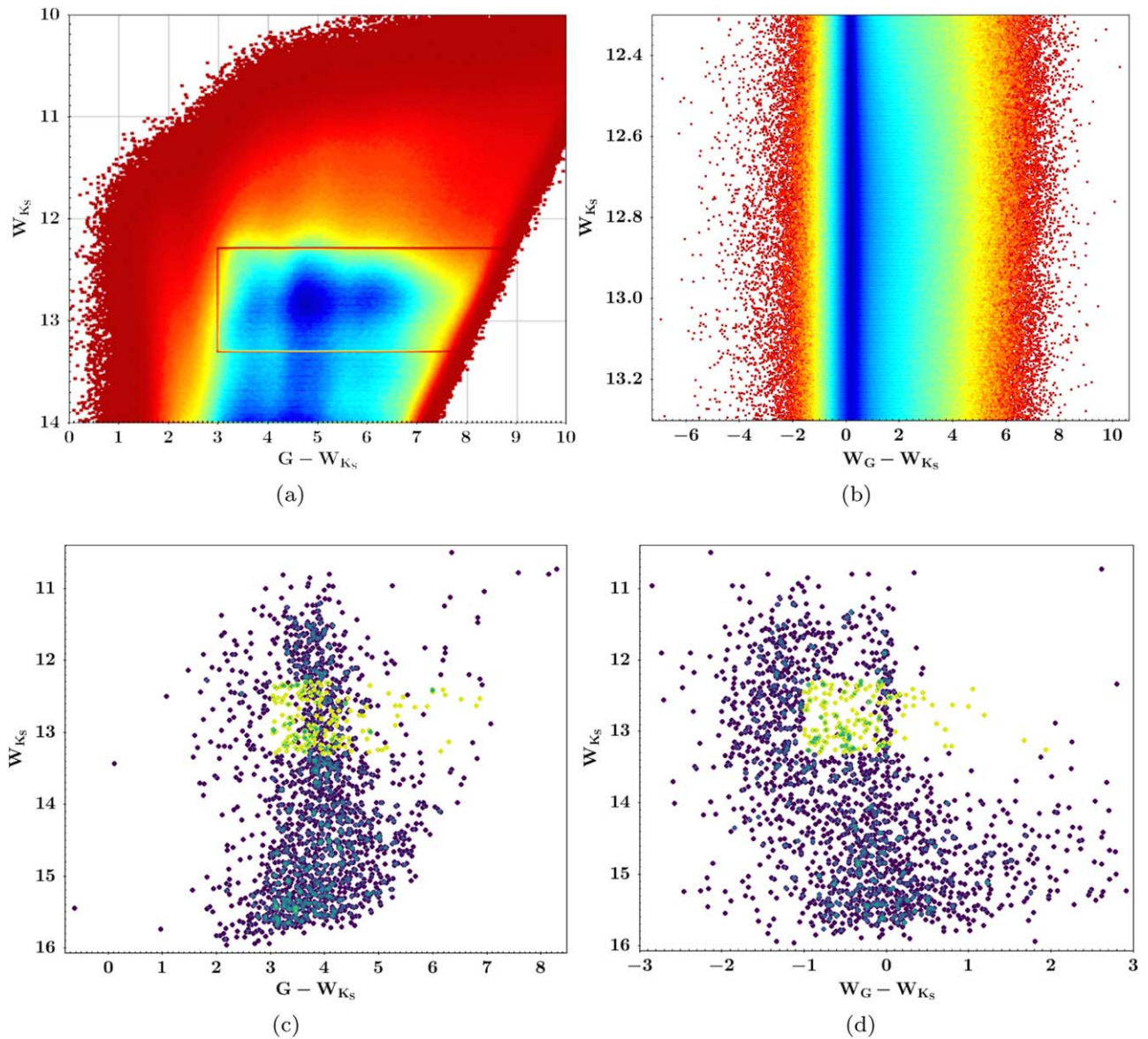

Figure 1. Near-IR CMD from VVV and *Gaia* using the reddening-independent Wesenheit magnitudes W_{K_S} and W_G. (a) The selection box used to single out bulge RC stars is shown. (b) Selected RC stars; from these, we select the ones in the range $-1 < (W_G - W_{K_S}) < 2$. (c) Same as subfigure (a), but with the new sample from the VVV, the green dots correspond to the color cut shown in an enclosed box in (a). (d) Using the Wesenheit magnitudes, we select the ones in the range $-1 < (W_G - W_{K_S}) < 2$.

$Z(0.87 \mu m)$, $Y(1.02 \mu m)$, $J(1.25 \mu m)$, $H(1.64 \mu m)$, and $K_S(2.14 \mu m)$.

The VVV Survey data reduction and the archival merging were carried out at the Cambridge Astronomical Survey Unit (CASU, Irwin et al. 2004) and VISTA Science Archive at the Wide-Field Astronomy Unit, within the VISTA Data Flow System (Cross et al. 2012).

In order to deal with the crowding in the VVV Survey field of view, we use the data set of Alonso-García et al. (2018), who built a new and more complete VVV photometric catalog using PSF photometry, which increased the number of detected sources up to almost a billion.

3. The Selection of Hypervelocity RC Stars

In order to select possible HVS candidates from the RC of the Bulge, we need to first define the appropriate region of the color–magnitude diagram (CMD) in different appropriate

colors where the RC lie. For that, and relying on the accuracy of the coordinates from both databases, we match the stellar position of the *Gaia* and VVV sources with a conservative tolerance of $0\rlap{.}''5$ (1.5 VVV pixels), resulting in a total of $N_{\text{total}} = 29,181,380$ sources that have accurate positions in the Galactic bulge region (within $-10° < l < 10°$, $-10° < b < 5°$), optical and near-IR photometry and PMs.

The Wesenheit magnitudes were originally created for Cepheids (Madore 1982), but they can be applied to any kind of star; we adopted them in our study since they are very successful in removing the reddening effect. The relations for the K_S and G band are, respectively, Equations (1) and (2):

$$W_{K_S} = K_S - 0.45 \times (J - K_S), \tag{1}$$

$$W_G = G - 1.90 \times (G_{BP} - G_{RP}). \tag{2}$$

We use the Wesenheit CMD in order to select RC stars. We apply color and magnitude cuts to the VVV CMD following

Table 1
Gaia and VVV Photometry of Bulge RC Stars

ID	Source ID[a]	R.A. (°)	Decl. (°)	Long (°)	Lat (°)	J (mag)	Ks (mag)	G_{DR1} (mag)
1	4043657695838288768	268.270	−31.751	−1.588	−2.827	14.195	13.261	17.252
2	4050119216276193152	272.291	−29.664	1.938	−4.809	13.949	13.138	16.265
3	4050891554627761536	273.355	−28.059	3.799	−4.865	13.670	12.873	15.649
4	4053940195338701056	265.668	−32.979	−3.776	−1.578	15.156	13.758	19.423
5	4055694466139424896	268.301	−31.314	−1.197	−2.629	14.253	13.015	17.639
6	4055974493662728064	267.280	−30.608	−1.037	−1.515	14.216	13.059	19.056
7	4056079565914165760	268.455	−30.941	−0.809	−2.554	14.583	13.622	17.471
8	4056243191160985728	269.922	−29.962	0.673	−3.159	13.587	13.242	16.723
9	4056355405826018688	267.689	−30.394	−0.673	−1.708	14.660	13.266	18.528
10	4056475218139133568	267.952	−29.386	0.311	−1.389	14.969	13.284	19.394
11	4056562732513987200	268.390	−29.274	0.602	−1.662	14.364	13.182	17.416
12	4056575308188029056	268.221	−29.192	0.598	−1.492	14.386	13.090	17.958
13	4056799093014910848	266.692	−30.180	−0.933	−0.860	15.229	13.534	18.118
14	4059583335633235456	262.454	−29.028	−1.929	2.870	14.657	13.518	17.850
15	4060422022558245248	264.260	−28.505	−0.629	1.824	14.508	13.059	18.390
16	4060809836556331648	266.370	−27.133	1.523	0.966	14.286	13.449	17.272
17	4060841348825794432	265.091	−27.820	0.342	1.570	14.440	13.056	18.432
18	4060858970977014784	264.922	−27.641	0.414	1.792	14.635	13.101	18.411
19	4060875566737607936	265.435	−27.529	0.751	1.465	14.635	13.150	18.714
20	4061174432075039488	263.213	−28.048	−0.742	2.847	14.549	13.226	18.031
21	4061331898466070528	264.003	−26.979	0.537	2.836	14.766	13.479	18.206
22	4061839842728015360	265.130	−26.232	1.708	2.382	14.882	13.755	18.312
23	4062483636849326080	270.111	−28.542	1.990	−2.599	13.669	13.292	16.562
24	4063159634713680384	271.092	−27.073	3.698	−2.631	14.063	13.172	16.617
25	4063179906906412032	270.221	−27.371	3.057	−2.104	13.836	12.953	16.805
26	4064174891897213312	270.357	−25.843	4.445	−1.454	14.355	13.167	19.434
27	4064524266009265024	272.582	−26.862	4.527	−3.691	13.633	13.082	16.970
28	4064649163703681792	273.736	−26.349	5.472	−4.354	15.235	13.838	17.394
29	4065639720555867904	271.476	−25.574	5.175	−2.200	14.668	13.502	17.806
30	4066241497024032768	272.943	−24.070	7.137	−2.639	14.442	13.195	17.934
31	4068160003069338112	265.081	−25.132	2.619	3.001	14.750	13.530	17.685
32	4089677381280701312	274.847	−22.935	8.968	−3.638	13.852	13.267	16.633
33	4110276761609748096	264.153	−24.768	2.479	3.908	13.421	12.976	17.491
34	4116316451998289664	264.374	−24.293	2.989	3.992	14.815	13.729	18.228

Note.
[a] Gaia DR2 ID.

Minniti et al. (2017) and similar color and magnitude cuts to the *Gaia* CMD. Combining *Gaia* G magnitude and VVV K_S magnitude, we construct a CMD and select the sources in the locus of the RC, shown enclosed in a box in Figure 1(a). From such sources, we select the ones in the range $−1 < (W_G − W_{K_S}) < 2$ in the CMD shown in Figure 1(b).

Now in order to select candidates with high proper motions in the inner Galaxy, from the VVV survey PSF catalog, we took the sources appearing in both studied epochs (2010 and 2015) and with observations in both J and K_S filters. The mean magnitude in K_S must be $K_S < 16$, in order to keep heavily reddened candidates, and maintain a constant magnitude between the two epochs in J and as well in K_S (mean magnitude–magnitude in a given epoch $< 3\sigma$). Differently from Alonso-García et al. (2018), now we also required that the sources had a spatial separation between both observation epochs of $0.''34 <$ tolerance $< 2.''5$, since the HVS candidates should show a larger separation between the observations.

We then match the stellar position of the *Gaia* DR2 and the second epoch of observation (2015) from the VVV sources with a tolerance of $0.''5$, resulting in a total of $N = 2752$ sources that, as before, have accurate positions in the Galactic bulge region ($−10° < l < 10°$, $−10° < b < 5°$), optical and

near-IR photometry and PMs. Figures 1(c) and (d) show the CMD for such a sample, where the light green points represent the RC stars, obtained from the same color cuts as explained before, shown in Figures 1(a) and (b). An exclusion for *Gaia* DR2 sources with well defined parallaxes must be done, we excluded those sources in which parallax error is less than 20%, placing them within 500 pc. Such procedure gives us a final sample of $N_{final} = 34$ RC stars.

In order to determine distances, we use the calibrations made by Ruiz-Dern et al. (2018) taking into account that the Wesenheit magnitudes are reddening-independent, so we can compute the absolute magnitudes as follows:

$$M_G = (0.495 \pm 0.009) + (1.121 \pm 0.128)(G − K_S − 2.1) \tag{3}$$

$$M_{K_S} = (−1.606 \pm 0.009) + (0.121 \pm 0.125) \\ (G − K_S − 2.1). \tag{4}$$

And in these cases, $G = W_G$ and $K_S = W_{K_S}$. It must be noted that the calibration for *Gaia* photometry described above is derived from *Gaia* DR1 and our data is from DR2, such photometric systems are different. Nevertheless, one can derive *Gaia* DR1 G magnitude from DR2 G magnitude following

Table 2
Wessenheit Magnitudes and Distance Estimations for the Bulge RC Stars

ID	Source ID[a]	W_{K_S} (mag)	$W_{G_{DR1}}$ (mag)	$M_{G_{DR1}}$ (mag)	$M_{W_{K_S}}$ (mag)	d_{K_S} (pc)	$d_{G_{DR1}}$ (pc)
1	4043657695838288768	12.841	12.485	−2.258	−1.903	8889.420	8885.327
2	4050119216276193152	12.772	12.978	−1.628	−1.835	8346.398	8342.555
3	4050891554627761536	12.514	12.642	−1.716	−1.845	7443.848	7440.421
4	4053940195338701056	13.129	14.806	0.021	−1.657	9061.674	9057.502
5	4055694466139424896	12.458	12.906	−1.357	−1.806	7124.595	7121.315
6	4055974493662728064	12.538	12.990	−1.352	−1.805	7389.867	7386.465
7	4056079565914165760	13.190	13.104	−1.955	−1.870	10283.742	10279.007
8	4056243191160985728	13.087	12.775	−2.209	−1.898	9929.270	9924.698
9	4056355405826018688	12.638	12.970	−1.487	−1.820	7791.625	7788.038
10	4056475218139133568	12.525	12.861	−1.482	−1.819	7394.923	7391.518
11	4056562732513987200	12.650	12.885	−1.596	−1.832	7877.056	7873.429
12	4056575308188029056	12.506	12.540	−1.821	−1.856	7454.419	7450.987
13	4056799093014910848	12.771	13.961	−0.525	−1.716	7897.280	7893.644
14	4059583335633235456	13.006	12.542	−2.379	−1.916	9646.467	9642.026
15	4060422022558245248	12.407	11.731	−2.617	−1.942	7409.066	7405.655
16	4060809836556331648	13.073	12.368	−2.649	−1.945	10082.708	10078.066
17	4060841348825794432	12.433	12.322	−1.984	−1.874	7267.601	7264.255
18	4060858970977014784	12.411	12.736	−1.495	−1.821	7020.124	7016.892
19	4060875566737607936	12.482	12.649	−1.672	−1.840	7317.010	7313.641
20	4061174432075039488	12.630	13.192	−1.229	−1.792	7663.788	7660.260
21	4061331898466070528	12.899	13.510	−1.174	−1.786	8650.874	8646.891
22	4061839842728015360	13.248	12.907	−2.242	−1.901	10712.555	10707.623
23	4062483636849326080	13.122	12.667	−2.369	−1.915	10171.570	10166.887
24	4063159634713680384	12.770	12.580	−2.072	−1.883	8523.819	8519.895
25	4063179906906412032	12.556	12.070	−2.403	−1.919	7850.388	7846.774
26	4064174891897213312	12.632	11.844	−2.742	−1.955	8269.080	8265.272
27	4064524266009265024	12.834	12.566	−2.160	−1.893	8818.134	8814.074
28	4064649163703681792	13.209	13.925	−1.056	−1.773	9918.750	9914.184
29	4065639720555867904	12.977	13.695	−1.054	−1.773	8911.397	8907.294
30	4066241497024032768	12.634	13.437	−0.959	−1.763	7574.675	7571.188
31	4068160003069338112	12.980	12.263	−2.663	−1.947	9670.046	9665.594
32	4089677381280701312	13.004	12.745	−2.150	−1.891	9528.832	9524.445
33	4110276761609748096	12.775	12.170	−2.538	−1.933	8743.221	8739.195
34	4116316451998289664	13.240	12.761	−2.396	−1.918	10756.680	10751.727

Notes.
[a] Gaia DR2 ID.

(Gaia Collaboration 2018):

$$G_{DR1} - G_{DR2} = -0.013612 - 0.079627(G_{BP} - G_{RP})$$
$$- 0.0040444(G_{BP} - G_{RP})^2 + 0.0018602$$
$$\times (G_{BP} - G_{RP})^3.$$

(5)

The distance in parsecs is:

$$d = 10^{(m_i - M_i + 5)/5}$$

(6)

where $m_i = W_{K_S}$; $W_{G_{DR1}}$ and $M_i = M_{K_S}$; $M_{G_{DR1}}$.

The RC giants are good distance indicators and allow us to define a volume limited sample. All of the 34 RC stars within $-10° < l < 10°$, $-10° < b < 5°$, lie within $6 < d < 11$ kpc.

With the distance estimation and using gala package (Price-Whelan 2017) from Astropy (Astropy Collaboration et al. 2013), we corrected the proper motions from Gaia DR2 ($\mu_{\alpha*} = \mu_\alpha \cos\delta$ and μ_δ) for the reflex motion of the Sun ($(u_\odot, v_\odot, w_\odot) = (11.1 ± 0.075, 245 ± 9, 7.25 ± 0.37)$ km s^{-1}), taking the default solar motion relative to the Galactic center as a combination for the peculiar velocity (Schönerich et al. 2010) and for the circular velocity at the solar radius (Bovy 2015). Given the corrected R.A. and decl. proper

motions, we transform to proper motions in Galactic coordinates ($\mu_{l*} = \mu_l \cos b$ and μ_b) with the same package.

While the Galactic coordinates have negligible errors, the individual distance errors are more difficult to estimate, because they are a combination of photometric errors, intrinsic RC error, and extinction errors. The photometric error for the typical RC magnitudes considered here is $\sigma K_S = 0.02$ mag (Saito et al. 2012). The error due to the intrinsic magnitude dispersion of the RC is $K_S = 0.009$ mag (Ruiz-Dern et al. 2018). The error from the extinction corrections depends on the slope of the adopted reddening law, and on the individual stellar reddening. Taking as a dereddened mean color $(J - K_S)_0 = 0.68$ (González et al. 2012), our RC sample yields $-0.335 < E(J - K_S) < 1.015$ mag. We estimate a typical total distance modulus error of $\sigma (m - M)_0 \approx 0.02$ mag, equivalent to $\sigma D \approx 0.38$ kpc at the distance of the bulge, adopted here to be $D_0 = 8.3$ kpc (Dekany et al. 2015).

We compute tangential velocities for all these stars using:

$$V_T (\text{km s}^{-1}) = 4.74 \times D(pc) \times \text{PM}(\text{arcsec yr}^{-1}),$$

where the distances are the ones estimated from Ruiz-Dern et al. (2018) using W_{K_S} magnitudes.
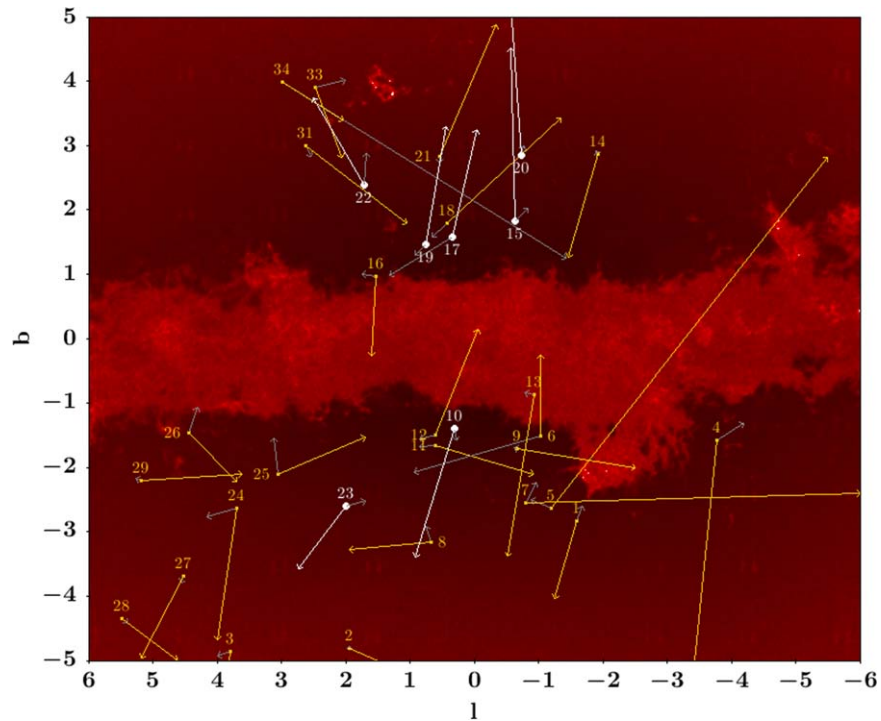
4

Figure 2. Density map of all RC sources with *Gaia* and VVV photometry. The red dots correspond to *Gaia* DR2 sources from the RC. The gray vectors show the *Gaia* PM (scaled five times so they can be visible), and the yellow vectors the VVV ones; they are labeled with their ID numbers. The white vectors represent the PMs derived from the VVV for the seven HVS candidates.

Table 3
Candidate Hypervelocity Bulge RC Stars

ID	Source ID[a]	Distance (pc)	PM[b] (mas yr^{-1})	V_T (km s^{-1})	T_{eject} (yr)
10	4056475218139133568	7394.923	208.743 ± 28	7317.575	24554.129
15	4060422022558245248	7409.066	269.609 ± 23	9469.333	25766.906
17	4060841348825794432	7267.601	171.367 ± 27	5903.893	33755.978
19	4060875566737607936	7317.010	185.743 ± 26	6442.689	31913.086
20	4061174432075039488	7663.788	493.208 ± 24	17918.229	21476.753
22	4061839842728015360	10712.555	156.447 ± 30	7944.791	67448.368
23	4062483636849326080	10171.570	123.374 ± 31	5948.829	95509.047

Notes. Tangential velocities and ejection times computed from VVV PMs.
[a] Gaia DR2 I.
[b] PM errors given that the NIR positional uncertainty for VVV amounts to 0.″08. Further information can be found at http://apm49.ast.cam.ac.uk/surveys-projects/vista/technical/astrometric-properties.

From the V_T equation it is clear that the errors in the tangential velocities are a combination of the distance errors described above, and the PM errors. Adopting typical *Gaia* PM errors at $G = 17$ mag of $\sigma PM = 0.2$ mas yr^{-1}, yields a mean error $\sigma V_T = 21.38$ km s^{-1}, using the K_S distance estimation for the sample.

The bulge is a very complicated region in terms of severe crowding and high reddening, and the optical *Gaia* PMs in this region may suffer from unknown errors. We note that the majority of the present stars are bright enough ($G < 20$ mag and $K_S < 14$ mag) so they should not be significantly affected by Poisson uncertainties.

We aim to locate HVS in the bulge ejected from the Galactic center, these would be HVS candidates ejected by binary interactions with the central SMBH (Hills 1988; Brown 2015). Therefore we select HVS candidates that appear to radiate from the Galactic center. For this, we project the PM vectors,

appropriately accounted for the solar motion, to be coming from a region within 2° (∼300 pc) from the Galactic center. This box of 2° was selected in order to account for errors in the individual PMs.

Accounting for the VVV derived PMs, we found seven stars that radiate from the Galactic center, whose IDs are 10, 15, 17, 19, 20, 22, and 23; their equatorial and Galactic coordinates, J, K_S, and G_{DR1} magnitudes are listed in Table 1; while their Wesenheit apparent and absolute magnitudes, as well as their distance estimations are listed in Table 2. As we have the stellar positions for the first epoch of observation in 2010 and the second one in 2015, we can derive the PM from the VVV data and compare these results with those of *Gaia* DR2. None of the stars that appear to radiate from the center concur in terms of the PMs from *Gaia* DR2 or derived from the VVV.

In order to verify if the usage of VVV derived PMs is a valid option, we have compared such PMs with *Gaia* DR2 PMs from

sources with a well-behaved astrometric solution, given by the astrometric excess noise and its significance (Lindegren et al. 2012). This comparison shows us that the *Gaia* and VVV PMs in this regime are comparable up to 95%, hence we can use these parameters to neglect the *Gaia* PM for those stars with significant astrometric excess noise and use the VVV more accurate PMs. The seven stars fulfill said condition, which makes them unreliable sources in terms of the astrometric solution from *Gaia* DR2; assuming that the PMs derived from the VVV data are accurate, we propose that these stars are HVS candidates, which are shown with white vectors in Figure 2.

4. Discussion

The spatial distribution shows that the candidate HVS with trajectories that point directly away from the Galactic center avoid the most reddened regions, but are concentrated to the plane (Figure 2). Taking into account that the on-going extension of the VVV survey (VVVX) will roughly double the areal coverage in the bulge, we can expect that the number of HVS that we will discover with the VVVX observations will also duplicate.

A qualitative comparison with models yields good agreement, because the models predict that the highest density of HVS would be in the bulge, closer to their production site. We found some excellent candidates that need to be followed-up. A more quantitative comparison can be left for the future because of the absence of radial velocities. The seven selected candidate hypervelocity RC stars (Table 3) are prime targets for radial velocity follow-up observations. The radial velocities would allow us to determine the orbits, in order to confirm if these are objects unbounded from the Milky Way.

In order to compute how long ago the HVS were ejected from the Galactic center, we use the negative PM vectors. We project the PM vectors backwards, in the direction toward the Galactic center, assuming that the modulus is correct and the direction is slightly off.

These times are listed in Table 3. Based on these times, we can estimate that there were at least seven stars ejected in the past $\sim 2.1 \times 10^4$ yr, or a rate of 3.26×10^{-4} stars yr^{-1}. This value is in agreement with the models of Zhang et al. (2013), that estimate ejection rates of 10^{-4}–10^{-5} stars yr^{-1} and with the rate adopted by Brown (2015) given the various theoretical results of 10^{-4} stars yr^{-1}.

It has been argued that there could be discrete episodes of ejections, as if, for example, a cluster of stars had a close encounter with the central SMBH (Capuzzo-Dolcetta & Fragione 2015; Fragione & Capuzzo-Dolcetta 2016); in our sample we can identify a major ejection episode, with HVS 10, 15, 17, and 19 ejected about 3×10^4 yr ago, followed by HVS 22 that has an ejection time of about 6.7×10^4 yr and HVS 23 with ejection 9.5×10^4 yr.

These admittedly crude results are based on small number statistics, and on assuming that the ejected stars travel at a constant velocity, so they should be taken with caution as first approximations. The acid test for this sample would be the measurement of radial velocities, that in combination with the distances and proper motions would give us the orbital parameters for the individual stars.

5. Conclusions

Bulge RC stars are ideal targets to search for HVS because they are numerous and their distances can be readily estimated. We obtained a bonafide sample of 34 bulge RC giants using near-IR data from the VVV Survey and optical data from *Gaia* DR2. Seven of these stars have PM vectors derived from the VVV consistent with being ejected from the vicinity of the the Galactic center that, despite *Gaia*PMs do not concur, have a significant astrometric excess noise within *Gaia* DR2 astrometric solution, making the *Gaia* PM unreliable, hence we propose these seven stars as HVS candidates. This would be the first detection of hypervelocity RC stars in the MW bulge.

Assuming that these candidate hypervelocity RC stars are real, we put limits on the total production rate of HVS from the Galactic center SMBH, obtaining $N_{HVRC} \sim 3.26 \times 10^{-4}$ yr^{-1} (i.e., one RC star ejected every about 3000 yr). Radial velocity follow-up observations are needed to confirm the hypervelocity RC star candidates, to estimate their orbital parameters, and to refine their times of ejection from the Galactic center.

New samples of HVS are needed for constraining the Galactic center ejection mechanism (Brown et al. 2018). This work shows that it is possible to find HVS in the bulge, close to their production site. If these stars are proven to be HVS, they would be the fastest ones found to date. It also represents the first step for mapping the distribution of bulge HVS. The recently started observations for the VVVX survey cover a larger area, significantly extending the map. Interestingly, the LSST (Ivezić et al. 2019) and the WFIRST (Spergel et al. 2015; Stauffer et al. 2018) would be promising future tools to identify even larger (perhaps by orders of magnitude) samples of bulge HVS and measure more precisely their production rate.

ORCID iDs

Alonso Luna ⓘ https://orcid.org/0000-0001-5971-8058
Dante Minniti ⓘ https://orcid.org/0000-0002-7064-099X
Javier Alonso-García ⓘ https://orcid.org/0000-0003-3496-3772

References

Alonso-García, J., Minniti, D., Catelan, M., et al. 2017, ApJL, 849, L13
Alonso-García, J., Saito, R. K., Hempel, M., et al. 2018, A&A, 619, A4
Astropy Collaboration, Robitaille, T. P., Tollerud, E. J., et al. 2013, A&A, 558, A33
Baumgardt, H., Gualandris, A., & Portegies Zwart, S. 2006, MNRAS, 372, 174
Boubert, D., Guillochon, J., Hawkins, K., et al. 2018, MNRAS, 479, 2789
Bovy, J. 2015, ApJS, 216, 29

Brown, W. R. 2015, ARA&A, 53, 15
Brown, W. R., Anderson, J., Gnedin, O. Y., et al. 2015, ApJ, 804, 49
Brown, W. R., Beers, T. C., Wilhelm, R., et al. 2008, AJ, 135, 564
Brown, W. R., Geller, M. J., & Kenyon, S. J. 2014, ApJ, 787, 89
Brown, W. R., Geller, M. J., Kenyon, S. J., & Kurtz, M. J. 2005, ApJL, 622, L33
Brown, W. R., Lattanzi, M. G., Kenyon, S. J., & Geller, M. J. 2018, ApJ, 866, 39
Capuzzo-Dolcetta, R., & Fragione, G. 2015, MNRAS, 454, 2677
Cross, N. J. G., Collins, R. S., Mann, R. G., et al. 2012, A&A, 548, 119
Dekany, I., Minniti, D., Hajdu, G., et al. 2015, ApJL, 799, L11
Emerson, J., & Sutherland, W. 2010, Msngr, 139, 2
Fragione, G., & Capuzzo-Dolcetta, R. 2016, MNRAS, 458, 2596
Fragione, G., Capuzzo-Dolcetta, R., & Kroupa, P. 2017, MNRAS, 467, 451
Fragione, G., & Loeb, A. 2017, NewA, 55, 32
Gaia Collaboration 2018, A&A, 616, A1
Geier, S., Fürst, F., Ziegerer, E., et al. 2015, Sci, 347, 1126
González, O. A., Rejkuba, M., Zoccali, M., et al. 2012, A&A, 543, A13
Heber, U., Edelmann, H., Napiwotzki, R., Altmann, M., & Scholz, R. D. 2008, A&A, 483, L21
Hills, J. G. 1988, Natur, 331, 687
Irrgang, A., Kreuzer, S., & Heber, U. 2018, A&A, 620, A48
Irwin, M., Lewis, J., Hodgkin, S., et al. 2004, Proc. SPIE, 5493, 411
Ivezić, Z., Kahn, S. M., Tyson, J. A., Abel, B., et al. 2019, ApJ, 873, 111
Kenyon, S. J., Bromley, B. C., Brown, W. R., & Geller, M. J. 2014, ApJ, 793, 122

Kollmeier, J. A., Gould, A., Knapp, G., & Beers, T. C. 2009, ApJ, 697, 1543
Lennon, D., van der Marel, R. P., Ramos Lerate, M., et al. 2017, A&A, 603, A75
Lindegren, L., Lammers, U., Hobbs, D., et al. 2012, A&A, 538, A78
Madore, B. F. 1982, ApJ, 253, 575
Marchetti, Contigiani, O., Rossi, E. M., et al. 2018, MNRAS, 476, 4697
Minniti, D., Contreras Ramos, R., Zoccali, M., et al. 2016, ApJL, 830, L14
Minniti, D., Lucas, P. W., Emerson, J. P., et al. 2010, NewA, 15, 433
Minniti, D., Saito, R. K., Gonzalez, O. A., et al. 2018, A&A, 616, 26
Minniti, D., Geisler, D., Alonso-García, J., et al. 2017, ApJL, 849, L24
Palladino, L. E., Schlesinger, K. J., Holley-Bockelmann, K., et al. 2014, ApJ, 780, 7
Price-Whelan, A. M. 2017, JOSS, 2, 18
Przybilla, N., Nieva, M. F., Heber, U., et al. 2008, A&A, 480, L37
Rossi, E. M., Kobayashi, S., & Sari, R. 2014, ApJ, 795, 125
Ruiz-Dern, L., Babusiaux, C., Arenou, F., Turon, C., & Lallement, R. 2018, A&A, 609, 116
Saito, R. K., Hempel, M., Minniti, D., et al. 2012, A&A, 537, A107
Schlafly, E., & Finkbeiner, D. P. 2011, ApJ, 737, 103
Schöenrich, R., Binney, J., & Dehnen, W. 2010, MNRAS, 403, 1829
Silk, J., Antonuccio-Delogu, V., Dubois, Y., et al. 2012, A&A, 545, L11
Spergel, D., Gehrels, N., Baltay, C., et al. 2015, arXiv:1503.03757
Stauffer, J., Helou, G., Benjamin, R., et al. 2018, arXiv:1806.00554
Yu, Q., & Tremaine, S. 2003, ApJ, 599, 1129
Zhang, F., Lu, Y., & Yu, Q. 2013, ApJ, 768, 153